Indian Journal of Geo Marine Sciences
Vol. 48 (07), July 2019, pp. 1008-1015

Experimental and simulation study on nonlinear pitch control of Seagull underwater glider

Daiwei Li[1], Junjun Cao[1], Chunhu Liu[1, 2], Zheng Zeng[1, 2*], Baoheng Yao[1, 2], & Lian Lian[1, 2*]
[1]The State Key Laboratory of Ocean Engineering, Shanghai Jiao Tong University, Shanghai 200240, China
[2]School of Oceanography, Shanghai Jiao Tong University, Shanghai 200240, China
*[E-mail: zheng.zeng@sjtu.edu.cn]

The Seagull underwater glider, developed by the Shanghai Jiao Tong University, is designed as a test-bed glider for the development and validation of various algorithms to enhance the glider's long-term autonomy. In this paper, an adaptive backstepping control (ABC) method is proposed for the nonlinear pitch control of the underwater glider gliding in the vertical plane. The linear quadratic regulator (LQR) control and proportional-integral-derivative (PID) control are applied and evaluated with the ABC method to control a glider in saw-tooth motion. Simulation results demonstrate inherent effectiveness and superiority of the LQR or PID based method. According to Lyapunov stability theory, the ABC control scheme is derived to ensure the tracking errors asymptotically converge to zero. The ABC controller has been implemented on Seagull underwater glider, and verified in field experiments in the Qiandao Lake, Zhejiang.

[Keywords: underwater glider; Adaptive control; underwater vehicle]

Introduction

As an ideal tool for ocean exploration, underwater gliders (UG) constitute a paramount advance in the highly demanding ocean monitoring scenario[1]. These slow-moving, long-endurance, compact, increasing robustness and buoyancy-driven vehicles can be used for a multitude of long-term oceanographic applications[2] or missions that are currently impossible to do using conventional, propeller-driven AUVs or moorings, and expensive if using research ships or towed vehicles[3]. Autonomous control and trajectory tracking are paramount part in a mission, requiring high reliability and robustness. Considering the operating mode of glider, attitude angles, especially pitch angle, would affect the stability and the safety of the whole glider system, making the control more complicated for glider, subject to modeling uncertainty[4,5] and ocean current disturbance[6,7]. Therefore it is crucial to develop an appropriate pitch control method to ensure the security and reliability of the glider system.

Generally, gliders rely on changes in vehicle buoyancy and internal mass redistribution for regulating their motion, do not carry thrusters or propellers and only have limited external moving control surfaces[8]. Therefore the dynamic model of the gliders is MIMO nonlinear system[9], which is under actuated and difficult to maneuver. Just because of complexity of the glider model, a multitude of oceanic gliders incorporate proportional-integral-derivative (PID) method control loops for regulating motion or for regulating a desired attitude[10].

To simplify the dynamic model of glider system, most references considered the glider vehicle as a particle[11, 12], especially in glider path planning research field. A phugoid mode approximation of underwater glider dynamics which is a representative case is formulated and controlled by laws derived through the Lyapunov based approach[13-15]. However, UG suffer from external disturbance, which leads the particle assumption to be too strict to misjudge. For improving the control and tracking precision, there are also some references that focused on the varying state variables of the system. Due to the analytical solution of the model in vertical plane, linear quadratic regulator (LQR) method was used to control and maintain the attitudes of gliders[10,16]. However, the control method only has exceedingly precise near the gliding equilibrium. The ABC method is used by Li[17] and Cao[18] to control the depth and pitch angle of glider, respectively; neural network controller method is also used in some research to predict and achieve the control inputs of the glider motion and the target outputs of the reference model[19].

Although there exists previous work of glider control and tracking, most of them only discussed

theory rather than realizing on prototype[20,21]. Due to the ABC's simple design procedure to stabilize system states by step-by-step recursive process, a nonlinear MIMO ABC method of underwater glider system is proposed in this paper. The comparison is made between ABC method simulations and experimental data for the glider model in vertical plane. The derivation process of the ABC method control formulas is described in detail, while a stable Lyapunov function is approached with global asymptotic stability. The comparisons of the simulation and experimental result demonstrate the effectiveness of the controller.

Dynamic Modeling

The glider dynamic model used in this study is adopted from an earlier work[22]. The equations in the dynamic model are nonlinear and coupled, and the system is underactuated with two inputs and three outputs, which is difficult to maneuver. Instead of showing the tedious and complex dynamic model, the state-space equations are established through reasonable simplification of the glider.

The definitions of all variables appearing in the dynamic model are: α is the angle of attack; m_1 and m_3 are the added mass along the body-1 and body-3 of vehicle, respectively; m_r is the internal moving mass; m_b is the ballast mass; J_2 is the added moment of inertia along the body-2 direction; g is the acceleration due to gravity; r_{p1} and r_{p3} are the positions of movable mass with respect to the center of buoyancy in body frame; v_1 and v_3 are the velocity components in body frame; θ is the pitch angle; ω_2 is the pitch rate; and K_{D0}, K_D, K_{L0}, K_L, K_{M0}, K_M, $K_{\omega_2^1}$ and $K_{\omega_2^2}$ are hydrodynamic parameters of the Seagull UG. The coefficients of this model are obtained by towing experiments introduced in Graver's work[23].

Some variables in the dynamic model are usually infinitesimal and have extremely limited effects to the dynamic of the glider while the glider operates at equilibrium. The following assumptions are made on these variables value:

Assumption 1. Neglect these coupled terms which include and in the equations.

By analyzing the equilibrium motion of underwater glider, the value of v_1 is always much bigger than the value of v_3, and the attack angle α is of usually small values, therefore the approximations.

Assumption 2. $v_1^2 + v_3^2 \approx v_1^2$, $\sin\alpha \approx v_3/v_1$.

Assumption 3. $\alpha \approx \sin\alpha$. The first term of Taylor expansion is taken which has high degree of approximation in this situation.

We apply the above assumptions to the dynamic model that describes the longitudinal dynamics of UG. The system can be rewritten in the following forms:

$$\dot{\theta} = \omega_2, \quad \ldots (1)$$

$$\dot{\omega}_2 = \frac{1}{J_2}\left(v_1 v_3 \left(m_3 - m_1 + K_M\right) - m_r g\left(r_{p1}\cos\theta + r_{p3}\sin\theta\right) + K_{M0} v_1^2 + K_{\omega_2^1}\omega_2 v_1^2\right), \quad \ldots (2)$$

$$\dot{v}_1 = \frac{1}{m_1}\left(-K_{D0} v_1^2 + K_{L0} v_1 v_3 - m_b g \sin\theta\right), \quad \ldots (3)$$

$$\dot{v}_3 = \frac{1}{m_3}\left(-K_{L0} v_1^2 - \left(K_L + K_{D0}\right) v_1 v_3 + m_b g \cos\theta\right), \quad \ldots (4)$$

$$\dot{r}_{p1} = u_1, \quad \ldots (5)$$

$$\dot{m}_b = u_2. \quad \ldots (6)$$

Control System Design

The flow chart of the nonlinear pitch control is shown in Figure 1, where the equilibrium solver is to obtain the equilibrium state of the system model. ξ_d and V_d are desired glide path angle and velocity, respectively. In this study, we use ABC method to design controller of the glider dynamics model, which is a two-input and three-output system.

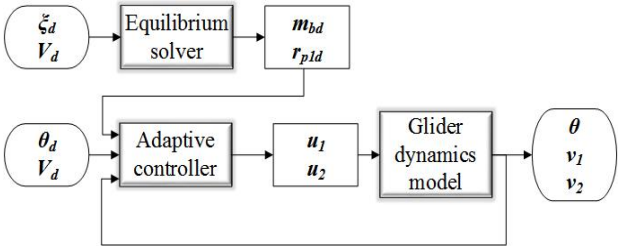

Fig. 1 — Block diagram with variables, control and dynamics

The ultimate goal of ABC method is to find a Lyapunov function and obtain a controller simultaneously. The derivative of the function should be nonpositive. We define

$$z_1 = \theta - y_{1d}, \quad \dots (7)$$

$$z_2 = \omega_2 - \mu_1, \quad \dots (8)$$

$$z_3 = v_1 - y_{2d}, \quad \dots (9)$$

$$z_4 = v_3 - \mu_2, \quad \dots (10)$$

$$z_5 = r_{p1} - \mu_3, \quad \dots (11)$$

$$z_6 = m_b - \mu_4, \quad \dots (12)$$

where y_{1d} and y_{2d} are desired outputs; $\mu_i\,(i=1,2,3,4)$ are estimations of the state variables.

Consider the following Lyapunov function candidate and the derivative

$$V = \sum_{i=1}^{6} \frac{1}{2} z_i^2, \quad \dots (13)$$

$$\dot{V} = \sum_{i=1}^{6} z_i \dot{z}_i \le 0. \quad \dots (14)$$

Remark 1. Contrary to general ABC, there are two inputs and two desired outputs in the system.

The two control inputs of the system can be established step-by-step as follow.

Step 1

The derivative of z_3 is

$$\dot{z}_3 = \dot{v}_1 - \dot{y}_{2d}, \quad \dots (15)$$

Define

$$\dot{v}_1 = z_6 - c_3 z_3, \quad \dots (16)$$

where c_3 is a constant value. Thus the expression of z_6 can be obtained:

$$z_6 = \frac{1}{m_1}\left(-K_{D0} v_1^2 + K_{L0} v_1 v_3 - m_b g \sin\theta\right) + c_3 z_3 - \dot{y}_{2d}, \quad \dots (17)$$

where, take a derivative of z_6 and choose

$$\dot{z}_6 = -c_6 z_6, \quad \dots (18)$$

where c_6 is a constant value. We can get the actual control law u_2 that can be formulated as follows:

$$u_2 = \frac{m_1\left(-c_6 z_6 + \ddot{y}_{2d} - c_3\left(z_6 - c_3 z_3\right)\right) + 2K_{D0} v_1 \dot{v}_1}{-g\sin\theta} \underline{\quad -K_{L0}\dot{v}_1 v_3 - K_{L0} v_1 \dot{v}_3 + m_b \dot{\theta} g \cos\theta}. \quad \dots (19)$$

Step 2

Consider with z_1 and define

$$\dot{z}_1 = z_2 - c_1 z_1, \quad \dots (20)$$

$$\dot{z}_2 = z_5 - c_2 z_2, \quad \dots (21)$$

$$\dot{z}_5 = -c_5 z_5, \quad \dots (22)$$

where c_1, c_2 and c_5 are constant values. The derivative of z_2 is

$$\dot{z}_2 = \frac{1}{I_{f2}}\left(v_1 v_3\left(m_3 - m_1 + K_M\right) - m_b r_{b1} g\cos\theta - m_r g\left(r_{p1}\cos\theta + R_p \sin\theta\right) + K_{M0} v_1^2 + K_q \omega_2 v_1^2\right) - \dot{y}_{1d} + c_1 \dot{z}_1, \quad \dots (23)$$

$$z_5 = \frac{1}{I_{f2}}\left(v_1 v_3\left(m_3 - m_1 + K_M\right) - m_b r_{b1} g\cos\theta - m_r g\left(r_{p1}\cos\theta + R_p \sin\theta\right) + K_{M0} v_1^2 + K_q \omega_2 v_1^2\right) - \dot{y}_{1d} + c_1 \dot{z}_1 + c_2 z_2, \quad \dots (24)$$

By taking derivative of z_5, we can get the actual control law u_1 that can be formulated as follows:

$$u_1 = \frac{\begin{array}{l} I_{f2}\left(-c_5 z_5 + \ddot{y}_{1d} - c_1 \ddot{z}_1 - c_2 \dot{z}_2\right) \\ -\left(\dot{v}_1 v_3 + v_1 \dot{v}_3\right)\left(m_3 - m_1 + K_M\right) \\ +\theta R_p m_r g\cos\theta + u_2 r_{b1} g\cos\theta \\ -\dot{\theta} m_b r_{b1} g\sin\theta - 2K_{M0} v_1 \dot{v}_1 \end{array}}{-K_q \dot{\omega}_2 v_1^2 - 2K_q \omega_2 \dot{v}_1 v_1 - r_{p1}\theta m_p g\sin\theta} \underline{\quad -m_r g\cos\theta}. \quad \dots (25)$$

Step 3

It is obvious from the above equations that the ultimate input control laws have no direct relationship to z_4. Therefore, define

$$z_4 = 0. \quad \dots (26)$$

The Lyapunov function of the whole system is

$$V = \frac{1}{2} z_1^2 + \frac{1}{2} z_2^2 + \frac{1}{2} z_3^2 + \frac{1}{2} z_5^2 + \frac{1}{2} z_6^2, \quad \dots (27)$$

$$\begin{aligned}\dot{V} &= z_1\dot{z}_1 + z_2\dot{z}_2 + z_3\dot{z}_3 + z_5\dot{z}_5 + z_6\dot{z}_6 \\ &= -c_1z_1^2 - c_2z_2^2 - c_3z_3^2 - c_5z_5^2 - c_6z_6^2 \\ &\quad + z_1z_2 + z_2z_5 + z_3z_6 \\ &\le \left(0.5-c_1\right)z_1^2 + \left(1-c_2\right)z_2^2 + \left(0.5-c_3\right)z_3^2 \\ &\quad + \left(0.5-c_5\right)z_5^2 + \left(0.5-c_6\right)z_6^2.\end{aligned} \quad \ldots (28)$$

By choosing the appropriate control parameters, $c_i\ (i=1,2,3,5,6)$ can make derivative of the Lyapunov function nonpositive at any time, which means the system is asymptotic stable. The nonlinear control of the glider system can be accomplished with the control law Eq. (19) and Eq. (25).

Simulation Results

To verify the performance of ABC method derived in this paper, linear quadratic regulator (LQR) control and PID control methods of the Seagull glider have been carried out and compared with the ABC method. Because the PID control method does not apply to the MIMO system, the equilibrium value m_b was used to be the constant value and the output is θ while v_1 and v_3 are considered to be unknown variables instead of systematic outputs.

The glider was moving first along the -45° downward glide and then switching to the 45° upward glide path, while the reference velocity is 0.4 m/s. The values of the control parameters are $c_1=0.5$, $c_2=1$, $c_3=0.5$, $c_5=0.5$, and $c_6=0.5$. The parameters of PID method used in this paper are: $K_P=-0.5$, $K_I=-0.08$, and $K_D=-0.67$. The state penalty Q and control penalty matrix R of LQR method in this case are chosen as

$$Q = diag(0.5,1,2,0.1,0.1,0.5), \quad \ldots (29)$$

$$R = diag(1,1). \quad \ldots (30)$$

Figure 2 demonstrates the comparison of output responses of the glider model by using the three

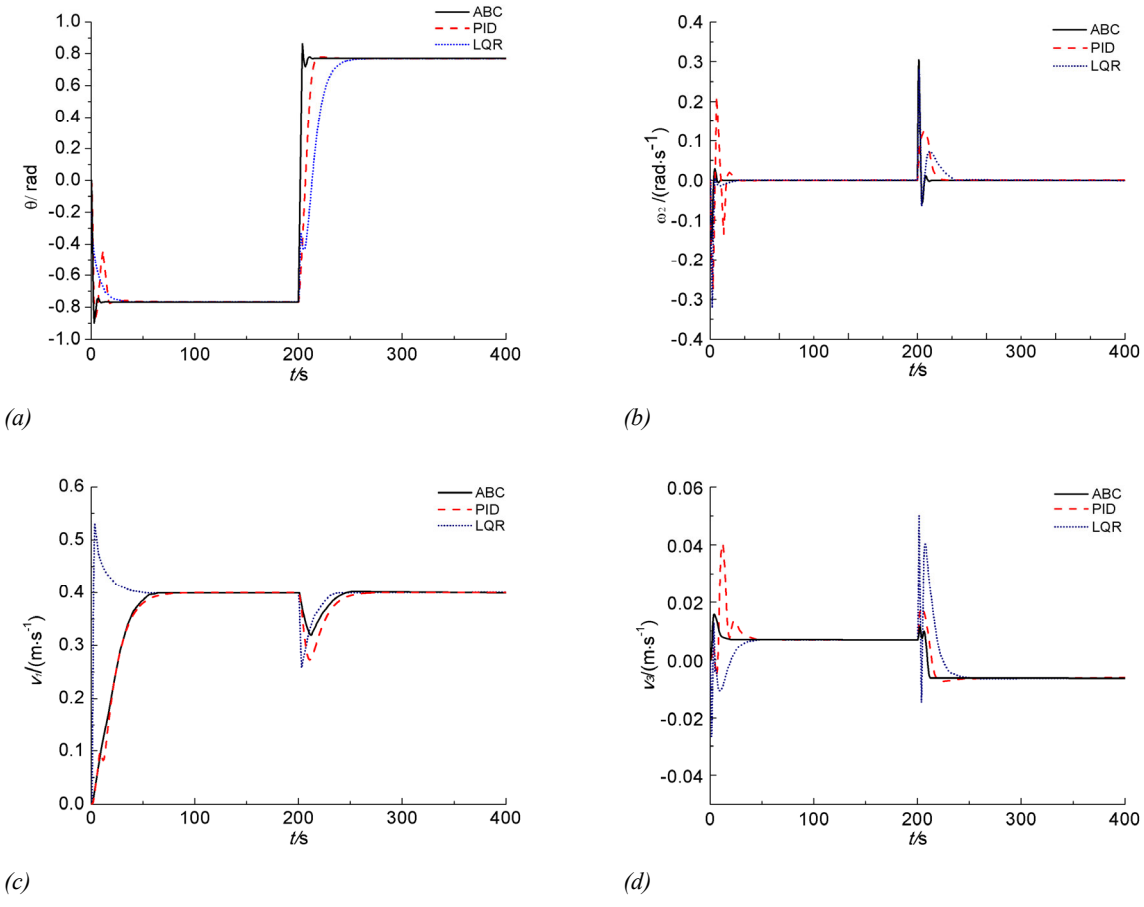

Fig. 2 — Output responses of Seagull dynamics with three control methods

control methods. It is obvious that the outputs converge to the desired equilibrium values, and the ABC method is able to restore the equilibrium state in a short time compared to the other two control methods. At the switching stage, the ABC method has smaller overshoot and is smoother than the PID and LQR. Therefore, the results of simulation have verified that the ABC method has a satisfactory performance in controlling the Seagull glider.

Prototype and Field Tests

This section presents the UG system and test set-ups used to investigate the nonlinear pitch control of UG.

UG system description

Seagull shown in Figure 3 is a fully functional UG designed for oceanographic research with 1 knot operating speed and six month duration. The glider comprises two basic payload packages, a class of vehicle shape (body of revolution with fixed special wings) and four subsystems (attitude control system, buoyancy control system, electrical system, and emergency release system). Energy use, cost, reliability, and ease of operation guided the design.

The hull length L and diameter D are 2.044 m and 0.231 m, respectively; more detailed specifications are provided in previous study of Cao[24].

The forward gliding motion of the glider is generated by the hydrodynamic lift force acting on a pair of wings. To fulfill the requirement of high speed, a pair of special wings with high lift-drag ratio is equipped on Seagull. The results of towing experiments and some data analysis were presented in other papers of Seagull[24].

The buoyancy control system is located at the head section of the pressure hull. To obtain accurate input of displacement volume of the glider during the experiment, we used an oil-tank instead of traditional external oil-bladder; and the improvement can provide accurate input by using a displacement sensor with relative tolerance to 10e-6 m.

Test set-up description and results

In July 2015, the Seagull glider was tested in Qiandao Lake. A series of gliding experiments, including saw-tooth motion and spiral motion, has been performed. The Seagull completed 22 diving cycles and reached the depth of 55 (the maximum operating depth of the testing area is 60 m). We present the experimental results collected for diving and rising five times during 1.3 h.

Since the scientific goal of this experiment was to explore how the pitch angle changes with the input and verify the efficiency of the ABC control method, we set the operational speed to 0.4 m/s and depth to 22 m as the same as simulation parameters. The nominal net buoyancy was set to neutral and the nominal position of the battery packages was at 0.09 m. When the glider dived and rose, the positions of the piston and the battery package were controlled by the desired attitudes of glider. And our ultimate

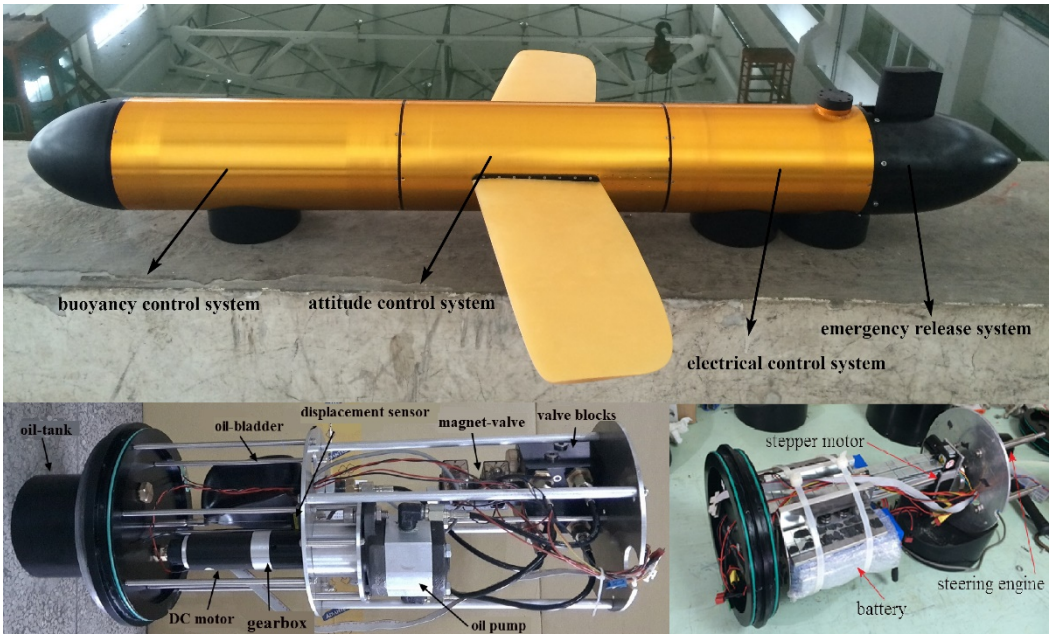

Fig. 3 — The distribution of Seagull UG with buoyancy control system and attitude control system

goal was to confirm whether the theoretical control law designed for the Seagull agreed with the experimental performance and the investigation we had done can be used to control the input for the glider.

During the course of the experiment, there existed a current with velocity V_c. The acoustic Doppler current profile (ADCP) was used to measure the velocity of the current, which was about 0.3 m/s. The velocity of the glider relative to the water was calculated and the velocity term in the dynamic model was replaced by the relative velocity. The comparison of experimental data collected and the simulation results were illustrated in Figure 4 and the experimental data was collected by the glider diving and rising five times. Because of the fluctuating and unstable current, we set the pitch angle to 10° and the depth to 22 m and the glider floated about 5 min to communicate with the base station when it rose up to the water surface. The depth of the glider was obtained by pressure sensor and the pitch angle was measured by flight control unit. The sampling frequency of pressure sensor and flight control reached 50 Hz.

As shown in Figure 4(a), the glider reached a maximum depth of 22 m; the pitch angle was approximately 10° as demonstrated in Figure 4(b). The experimental results implied that the gliding motion was greatly influenced by the fluctuating currents mainly at the switching stage and on the water surface. The comparisons obviously demonstrated that there existed a phase shift between the experimental collected data and simulation results while the phase shift was generated by the clock setting on the microcomputer. Every time the glider rose up to the surface, we draw the GPS data on the lake map, and then we got the track of the glider as shown in Figure 5.

Additionally, there are some other factors that may have contributed to the difference between experimental collected data and simulation results.

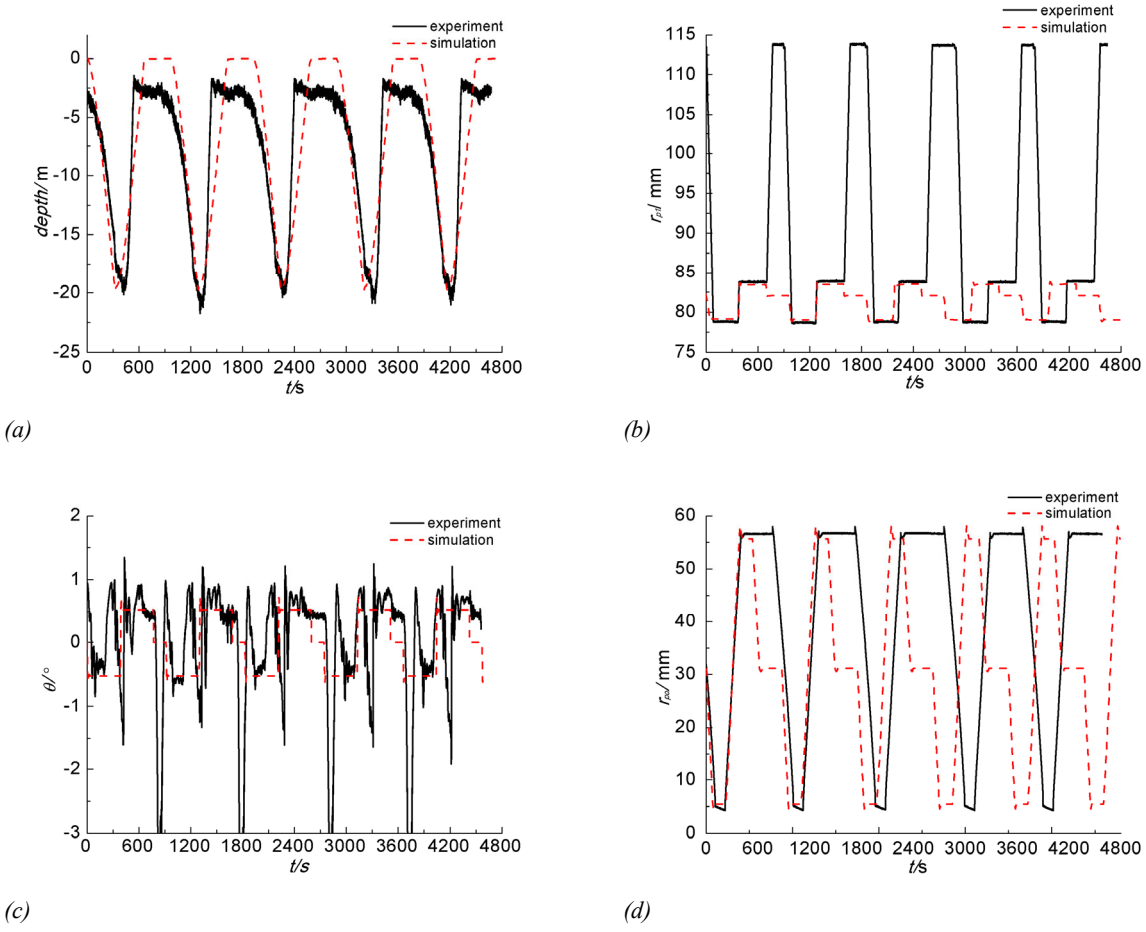

Fig. 4 — Comparing experimental results with simulation results

Fig. 5 — The GPS values of the glider during the experiment

These various masses of the glider are treated as rigid material point in the glider dynamic model, while the shape of the glider was described by the hydrodynamic coefficients obtained by towing experiment or numerical computation. In the actual system, the net-buoyancy is controlled by pumping oil between bladder and oil-tank; the other static mass and movable mass were distributed inside the glider, which makes it difficult to determine the distribution accurately; the hydrodynamic coefficients of glider are usually uncertain and different to obtain, and the coefficients used in the simulation are hard to precise the experiment conditions, such internal and external frictions and external disturbances. All the uncertainties or time-varying factors could affect the system's performance and make the experimental data different from the simulation results. However, in these comparison figures, the simulating results are in accordance with the results of experiment, which offers convincing evidence that the ABC controller captures the inputs and adjusts the pitch angle of the glider to a satisfactory accuracy level.

Conclusion

This paper presented a new approach for nonlinear MIMO control of underwater glider systems in vertical plane. The adaptive control laws were derived according to Lyapunov stability theory. The ABC controller was implemented on Seagull underwater glider and verified in field experiments. Among the simulation results of three control methods, the ABC method manifested the best performance. The experimental data collected using sensors as well as results from MATLAB simulations provided that the derived adaptive backstepping nonlinear controller can capture the inputs of the glider to a satisfactory level. Therefore, we conclude that the ABC controller can be used to control the glider in practice in saw-tooth motion, in three dimensions.

Acknowledgment

The authors gratefully acknowledge the support from Xiaochao Zhang, Wei Ping and Yuqian Li at Shanghai Jiao Tong University who made indispensable contribution to this work.

References

1 M. Brito, D. Smeed, and G. Griffiths, Underwater Glider Reliability and Implications for Survey Design, *J. Atmos. Ocean. Technol.*, 31. 12(2014) 2858–2870.

2 D. L. Rudnick, R. E. Davis, C. C. Eriksen, D. M. Fratantoni, and M. J. Perry, Underwater Gliders for Ocean Research, *Mar. Technol. Soc. J.*, 38.2(2004) 73–84.

3 Z. Zeng, L. Lian, K. Sammut, F. He, Y. Tang. A survey on path planning for persistent autonomy of autonomous underwater vehicles. *Ocean Eng.*, 110(2015) 303-313.

4 M. Nakamura, K. Asakawa, T. Hyakudome, S. Kishima, H. Matsuoka, and T. Minami, Study on hydrodynamic coefficients of underwater vehicle for virtual mooring, *2011 IEEE Symp. Underw. Technol. Work. Sci. Use Submar. Cables Relat. Technol.*, (2011) 1–7.

5 Qin Zhang, Jialei Zhang, Ahmed Chemori, Xianbo Xiang. Virtual Submerged Floating Operational System for Robotic Manipulation. *Complexity*, (2018) 1–18.

6 J. Cao, Z. Zeng, L. Lian. Dynamics and approximate semi-analytical solution of an underwater glider in spiral motion. *Indian Journal of Geo-Marine Sciences*, 44.12(2015) 1833-1839.

7 S. Fan and C. a. Woolsey, Dynamics of underwater gliders in currents, *Ocean Eng.*, 84(2014) 249–258.

8 N. A. A. Hussain, M. R. Arshad, and R. Mohd-Mokhtar, Underwater glider modelling and analysis for net buoyancy, depth and pitch angle control, *Ocean Eng.*, 38.16(2011) 1782–1791.

9 J. Cao, J. Cao, Z. Zeng, L. Lian, Nonlinear multiple-input-multiple-output adaptive backstepping control of underwater

glider systems, *International Journal of Advanced Robotic Systems*, 13.6(2016) 172988141666948.

10 N. Mahmoudian and C. Woolsey, Underwater glider motion control, *2008 47th IEEE Conf. Decis. Control*, (2008) 552–557.

11 E. E. Heslop, S. Ruiz, J. Allen, J. L. López-Jurado, L. Renault, and J. Tintoré, Autonomous underwater gliders monitoring variability at "choke points" in our ocean system: A case study in the Western Mediterranean Sea, *Geophys. Res. Lett.*, 39.20(2012) L20604.

12 Caoyang Yu, Xianbo Xiang, Lionel Lapierre, Qin Zhang. Robust magnetic tracking of subsea cable by AUV in the presence of sensor noise and ocean currents. *IEEE Journal of Oceanic Engineering*, 43.2(2018) 311–322.

13 P. Bhatta and N. E. Leonard, Nonlinear gliding stability and control for vehicles with hydrodynamic forcing, *Automatica*, 44.5(2008) 1240-1250.

14 Zhenzhong Chu, Xianbo Xiang, Daqi Zhu, Chaomin Luo, De Xie. Adaptive Fuzzy Sliding Mode Diving Control for Autonomous Underwater Vehicle with Input Constraint. *International Journal of Fuzzy Systems*, 20.5(2018) 1460-1469.

15 Caoyang Yu, Xianbo Xiang, Philip A. Wilson, Qin Zhang. Guidance-error-based robust fuzzy adaptive control for bottom following of a flight-style AUV with saturated actuator dynamics. *IEEE Transactions on Cybernetics*, 99(2018) 1-13.

16 Z. Zeng, A. Lammas, K. Sammut, F. He, Y. Tang. Shell space decomposition based path planning for AUVs operating in a variable environment. *Ocean Eng.*, 91 (2014) 181-195.

17 J.-H. Li and P.-M. Lee, Design of an adaptive nonlinear controller for depth control of an autonomous underwater vehicle, *Ocean Eng.*, 32. 17–18(2005) 2165–2181.

18 J. Cao, B. Yao, L. Lian. Nonlinear pitch control of an underwater glider based on adaptive backstepping approach, *J. Shanghai Jiao Tong Univ.*, 20. 6(2015) 729–734.

19 K. Isa and M. R. Arshad, Neural Networks Control of Hybrid-Driven Underwater Glider, *Oceans IEEE*, (2011) 2–8.

20 J. Cao, J. Cao, Z. Zeng, B. Yao, L. Lian. Toward Optimal Rendezvous of Multiple Underwater Gliders: 3D Path Planning with Combined Sawtooth and Spiral Motion. *J. Intelligent & Robotic Systems*, 85(2017) 1-18.

21 P. Bhatta, Nonlinear stability and control of gliding vehicles, *Recent Developments in Ruminant Nutrition*, 4(2006) 325–352.

22 S. Zhang, J. Yu, A. Zhang, and F. Zhang, Spiraling motion of underwater gliders: Modeling, analysis, and experimental results, *Ocean Eng.*, 60(2013) 1–13.

23 J. G. Graver and N. E. Leonard, Underwater glider dynamics and control, *12Th Int. Symp. Unmanned Untethered Submers. Technol.*, (2001) 1742–1710.

24 J. Cao, J. Cao, Z. Zeng, B. Yao, and L. Lian, Seagull — Designed for Oceanographic Research. *Oceans IEEE*, (2016) 1-7.